Sampling-dependent systematic errors in effective harmonic models

E. Metsanurk* and M. Klintenberg
Department of Physics and Astronomy, Uppsala University, Box 516, S-75120 Uppsala, Sweden

(Received 28 February 2019; revised manuscript received 25 April 2019; published 28 May 2019)

Effective harmonic methods allow for calculating temperature-dependent phonon frequencies by incorporating the anharmonic contributions into an effective harmonic Hamiltonian. The systematic errors arising from such an approximation are explained theoretically and quantified by density-functional-theory-based numerical simulations. Two techniques with different approaches for sampling the finite-temperature phase space in order to generate the force-displacement data are compared. It is shown that the error in free energy obtained by using either can exceed that obtained from 0 K harmonic lattice dynamics analysis, which neglects the anharmonic effects.

DOI: 10.1103/PhysRevB.99.184304

I. INTRODUCTION

The harmonic approximation of the potential energy is a fundamental part of the analysis of vibrational properties of materials in both theoretical and experimental studies [1]. Its usefulness is multifold in the sense that not only does it allow for capturing the dominant part of the potential energy surface, but it makes deriving exact analytical relations for all temperature-dependent vibrational thermodynamic properties possible. In addition, the harmonic system can be used as a reference point for either integration- or perturbation-based methods in order to find the corrections due to anharmonicity that always exists in real systems.

The lattice dynamics approach [2] to calculate the normal vibrational modes of a crystal can break down either when very strong quantum-mechanical effects dominate, as is the case for crystalline helium [3], or, more commonly, due to mechanical instabilities, for example, cubic zirconia [4] or titanium, zirconium, and hafnium in the bcc structure [5]. This results in some of the normal modes having imaginary vibrational frequencies due to a decrease in the total potential energy when the atoms are displaced along those modes. The integrals over the whole normal-mode space, which define the harmonic free energy and all the other derived thermodynamic properties, are in that case complex-valued and the properties are thus commonly interpreted as undefined.

Recently, methods have been proposed to calculate free energies of such systems for cases where the lattice is dynamically unstable [6] or stabilized due to temperature [7]. Both are based on partitioning of atomic configuration space, calculating the free energy of each region separately, and adding those energies together, consistent with equilibrium thermodynamics.

Instead of the aforementioned detailed mapping, it is also possible to fit high-temperature force-displacement data obtained from atomistic simulation to a truncated expansion of the potential energy surface, after which the second-order effective force constants can be used to calculate the temperature-dependent phonon frequencies and hence the effective harmonic free energy. This is the basis for the methods of self-consistent *ab initio* lattice dynamics (SCAILD) [5,8,9] and temperature-dependent effective potential (TDEP) [10–12]. Neither is inherently limited to being used for analyzing only systems with dynamical instabilities, which could be considered the most severe case, so both can be used to treat any kind of anharmonicity.

Currently, the best way to gather the data for either of the methods is through density functional theory (DFT) [13], which, in principle, provides a parameter-free way to explore the dynamics of realistic, as opposed to model, systems. *Ab initio* based thermodynamics has been shown to be a promising way to predict the thermal properties of materials taking all the relevant excitations, not limited to vibrational ones, into account [14,15].

Without considering whether DFT with its approximations can provide reliable enough data, there are also other systematic and statistical uncertainties associated with calculating thermodynamic properties. Some of those, such as the limited system size, can be partially dealt with by Fourier interpolating the information about vibrations in an infinite crystal [4], while others, such as the limited amount of time for sampling, can be dealt with by upsampled thermodynamic integration with Langevin dynamics (UP-TILD) or harmonically mapped averaging [16,17]. Regardless of the method used, the total uncertainty required to produce satisfactory results is often under 1 meV/atom. For example, a 6 meV/atom shift on the energy scale results in 400 K (60%) overestimation of the fcc to bcc transition temperature for calcium using *ab initio* calculations [18].

Given the requirement of high accuracy for any method used to calculate thermodynamic properties, it is necessary to understand how the models behave under certain conditions. In this study we analyze the accuracy of effective harmonic models by comparing SCAILD and TDEP both theoretically and numerically at different temperatures. It has been shown that effective harmonic methods do not necessarily give a significant improvement over 0 K harmonic approximation

*erki.metsanurk@physics.uu.se

[19] and that the difference between the free energies predicted by the two methods increases with temperature [20]; however, no theoretical explanation was provided regarding what in particular could cause the discrepancy between these two very similar models.

II. METHODOLOGY

A. Harmonic approximation at 0 K and finite temperatures

In order to simplify the comparison of the two methods a slight reformulation of the theory is needed compared to that described in the original works. The starting point is the force-displacement relation through a $3N \times 3N$ force constant matrix Φ, so for any atomic configuration c the forces are given by

$$\vec{f}_c = -\Phi(\vec{\theta})\vec{u}_c. \tag{1}$$

In a similar fashion to Hellman *et al.* [11], the elements of Φ are expressed as linear combinations of parameters $\vec{\theta}$ as the force constants of crystalline systems are, in general, not independent but constrained by rotational, translational, and inversion symmetry of the lattice and by the requirement that force appears on any atom under rigid translation of the whole crystal. For the supercell used in this study, the number of force constants is reduced from 82944 to 52.

This allows us to rewrite Eq. (1) as

$$\vec{f}_c = C(\vec{u}_c)\vec{\theta}. \tag{2}$$

where the elements of matrix C_c are linear combinations of displacements, the coefficients of which depend on the choice of the supercell and the aforementioned symmetry constraints. The parameters $\vec{\theta}$ can now be found with the linear least-squares method using the Moore-Penrose inverse of C,

$$\vec{\theta} = C^{+}(\vec{u})\vec{f}, \tag{3}$$

where we have omitted the indices c since both $\vec{f}$ and $\vec{u}$ can contain the forces and displacements of any number of atomic configurations. The more anharmonic the system is, the more configurations are needed in order to keep the uncertainty of the fit sufficiently small. By expressing $\vec{\theta}$ as a function of temperature we obtain a temperature-dependent effective harmonic force constant matrix from which the phonon frequencies and eigenvectors can be calculated.

When working only with the vibrational modes commensurate with the supercell, it is more convenient to consider the supercell itself to be the unit cell and calculate the exact normal-mode frequencies which correspond to $\vec{q} = (0, 0, 0)$, i.e., only at the Γ point of the reciprocal lattice of the supercell. In that case the dynamical matrix for the whole system is

$$D = M^{-\frac{1}{2}}\Phi(\vec{\theta})M^{-\frac{1}{2}} = Q(\vec{\theta})\Omega^2(\vec{\theta})Q^T(\vec{\theta}), \tag{4}$$

where M is a diagonal matrix of the masses of the atoms, Ω^2 is a diagonal matrix of eigenvalues, and Q is a matrix whose columns are the eigenvectors.

By substituting Eq. (4) into Eq. (1) we get the following general equation that applies to both SCAILD and TDEP:

$$Q^T(\vec{\theta})M^{-\frac{1}{2}}\vec{f}_c = -\Omega^2(\vec{\theta})Q^T(\vec{\theta})M^{\frac{1}{2}}\vec{u}_c. \tag{5}$$

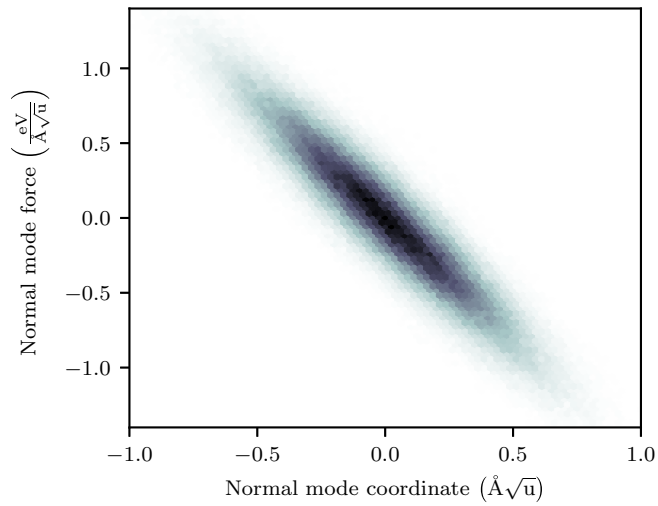

FIG. 1. A histogram of the force-displacement relation for a single phonon mode extracted from a molecular dynamics simulation at 1600 K. The darker areas correspond to higher-probability states. A linear fit through the distribution gives the negative square of the effective mode frequency.

One of the approximations of SCAILD is that the eigenvectors are temperature independent and can thus be obtained from a quick 0 K phonon calculation. Whether this holds depends on the symmetry properties of the system and the choice of the supercell, which determines the grid of sampled q points [21]. For the system considered in this work, this approximation does not have significant effect on the results.

Equation (5) then becomes

$$\vec{\phi}_c = -\Omega^2\vec{v}_c, \tag{6}$$

where $\vec{\phi}_c = Q^T M^{-\frac{1}{2}}\vec{f}_c$ is the normal-mode force and $\vec{v}_c = Q^T M^{\frac{1}{2}}\vec{u}_c$ is the normal-mode displacement. The $\vec{\theta}$ dependence is removed since we are interested in Ω, which can be obtained from a simple linear least-squares fit, and how its elements are related to the parameters becomes irrelevant.

For a perfectly harmonic crystal there exists one and only one Ω^2. For anharmonic crystals, however, the uniqueness is lost due to the higher-order terms in the Hamiltonian becoming relevant. A typical distribution of the normal-mode force-displacement relation for a single phonon mode is depicted in Figs. 1 and 2. The shape is that of a Gaussian due to both the nature of constant-temperature sampling of the configurations and the anharmonicity of the system. The modes that are symmetrically equivalent can be placed on the same plot, thereby increasing the amount of data, thereby reducing the uncertainty of the linear fit and retaining the symmetry properties of the vibrations.

As we have shown, TDEP is mathematically equivalent to SCAILD for systems with temperature-independent phonon eigenvectors. The linear least-squares fit is done in real space for the former and in normal-mode space for the latter.

Our approach differs slightly from the original formulation of SCAILD where sampling of the normal-mode displacements, in order to obtain the forces, was limited to certain discrete values that give the same mean-square displacement as a quantum harmonic oscillator at a constant temperature,

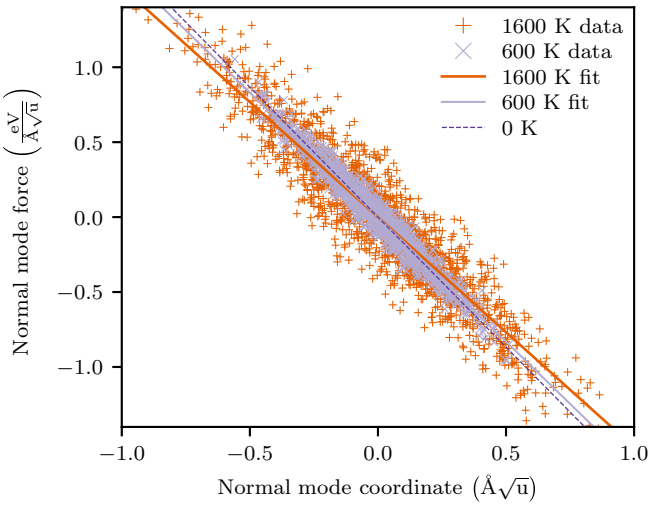

FIG. 2. A typical force-displacement plot for a single frequency but symmetrically equivalent phonon modes for illustrating and fitting effective harmonic models. Not all points are shown for visualization purposes. As the temperature increases, the distribution of forces for fixed displacements broadens. The frequency of the mode is 20.6, 20.1, and 19.4 THz at 0, 600, and 1600 K, respectively.

i.e.,

$$\vec{u} = M^{-\frac{1}{2}} Q \vec{d}, \tag{7}$$

where

$$d_i = \pm \sqrt{\frac{\hbar}{\Omega_{i,i}} \left[\frac{1}{2} + \left(\exp \frac{\hbar \Omega_{i,i}}{k_B T} - 1 \right)^{-1} \right]}. \tag{8}$$

That makes it possible to take the average of Ω^2 over all the sampled configurations, which means the average slope of all the lines from the origin to every point in the force-displacement plot. This is not mathematically equivalent to a linear least-squares fit through all the points. In addition, when the displacements for SCAILD are sampled from a Gaussian distribution, as done in this work, the most likely displacement for a given mode is zero, while the force due to the anharmonicity is nonzero, which leads to many large positive and negative Ω^2 values which are not likely to cancel out, leading to a large error in the estimation of the average value.

B. Sampling of the configuration space

The major difference between TDEP and SCAILD is the way the displacements are obtained. For TDEP it is a constant-temperature molecular dynamics simulation consistent with the Hamiltonian of the anharmonic system, whereas for SCAILD the displacements are sampled from the distribution self-consistent with the current best-fit harmonic Hamiltonian. The major advantage of the latter is the reduction in the number of calculations due to more efficient generation of uncorrelated samples as there exists an analytical expression that gives correct constant-temperature statistics.

Using the samples generated by a canonical molecular dynamics or Monte Carlo simulation can be interpreted as finding the harmonic potential that reproduces the forces given by the anharmonic Hamiltonian for constant temperature with the smallest error in least-squares sense. It is not unlike using the method of force matching quite commonly employed in order to fit empirical interatomic potentials to DFT reference data [22]. The lack of transferability is often an issue with empirical potentials, and as we explain below, it also plays an important role in the effective harmonic models.

It is slightly less obvious what the sampling used in SCAILD method yields. In addition to the resulting model being harmonic, the displacements themselves are generated assuming noninteracting phonon modes. It has been suggested that this results in probing the wrong parts of the phase space [23], which is certainly true when the actual anharmonic system is concerned; however, the goal here is not to perfectly reproduce the whole anharmonic Hamiltonian but to pack the anharmonic vibrational information into a truncated Taylor expansion of the potential. Nevertheless, by careful reasoning, one can identify the possible effects of the harmonic sampling when compared to the anharmonic one. Since in the former case all the correlations in the motion of the normal modes are ignored, the probability of sampling higher-energy configurations increases, which results in larger magnitudes for the sampled forces and in turn higher effective vibrational frequencies which increase with temperature.

While it is clear that the two sampling methods are different, it does not automatically follow that one provides a better free-energy estimation than the other. In both cases we obtain a harmonic Hamiltonian, both of which are just approximations and so are the predicted free energies. While there might exist an effective harmonic model that gives the exact free energy of the system, it is not immediately clear whether either of the methods should do that.

C. Thermodynamic integration and free-energy perturbation

Since we expect SCAILD and TDEP to give different harmonic force constant matrices and therefore also different free energies, the full vibrational free energy needs to be calculated for a proper comparison. Both methods provide an excellent reference system for free-energy perturbation (FEP) and thermodynamic integration (TI) when compared to the Einstein crystal [24,25], which has a smaller overlap with the phase space of the anharmonic system, and to a 0 K harmonic model [26,27], which has undefined free energy in the case of phonon modes with imaginary frequencies. It must be noted that the efficiency of thermodynamic integration can be increased even more by using an intermediate potential, such as a local anharmonic one [28], a semiempirical one [29], or one based on machine learning [19].

Both FEP and TI allow us to calculate free-energy differences from ensemble averages of energy differences. There are several variations of each. In this work we used a linear path through a parameter λ from the effective harmonic system to the anharmonic one, in our case a DFT system as follows:

$$U(\lambda) = \lambda U_{\mathrm{DFT}} + (1 - \lambda) U_{\mathrm{EH}}. \tag{9}$$

To get the free-energy difference from thermodynamic integration we calculate

$$\Delta F = \int_0^1 \left\langle \frac{\partial U(\lambda)}{\partial \lambda} \right\rangle_\lambda d\lambda = \int_0^1 \langle U_{\mathrm{DFT}} - U_{\mathrm{EH}} \rangle_\lambda d\lambda. \quad (10)$$

In practice there are possibilities either to sample λ on a discrete, but not necessarily equidistant, grid or to perform adiabatic switching where λ changes continuously throughout the simulation.

Since SCAILD and TDEP sample a lot of configurations and provide both the harmonic and DFT energies, it is also, in principle, possible to calculate the anharmonic free energy without any extra steps through free-energy perturbation:

$$\Delta F = (-1/\beta) \ln \langle \exp[-\beta(U_B - U_A)] \rangle_A \quad (11)$$

For TDEP, U_A are the potential energies from a DFT molecular dynamics (MD) calculation, and U_B are the potential energies calculated using the fitted harmonic model. For SCAILD, U_A are the harmonic potential energies calculated using the converged fit, and U_B are the potential energies for the same structures obtained from DFT. FEP can also be done using stratified calculations. Similar to thermodynamic integration, several intermediate simulations using mixed Hamiltonians of the two end points can be done, and the free-energy differences between each step can be calculated using Eq. (11) and subsequently summed together [30].

D. Calculations

Cubic zirconia was chosen for the system to be studied for several reasons. It has been studied using 0 K [4], self-consistent lattice dynamics [8], and other methods [31]. At ambient pressure it is not dynamically stable, as indicated by the large number of imaginary phonon modes which disappear when a SCAILD analysis is performed. Another option for achieving dynamical stability for cubic ZrO_2 is to put it under high pressure, which we opted to do in order to retain the ability to compute the free energy from the 0 K phonon calculation for comparison.

As explained above, the theory simplifies a lot in cases where the eigenvectors can be assumed not to depend on temperature. ZrO_2 contains two types of atoms with a relatively large difference in atomic weights, which should theoretically allow for the possibility of temperature-dependent eigenvectors. The size of the supercell was chosen to be $2 \times 2 \times 2$ of the conventional unit cell with a lattice parameter of 9.7 Å, containing a total of 96 atoms. It is not guaranteed to give a converged free energy with respect to the size but is a good balance between capturing the overall vibrational, both harmonic and anharmonic, behavior while allowing for sufficiently long molecular dynamics simulations.

All phonon calculations were done using PHONOPY [2] without applying a nonanalytical term correction. For SCAILD and TDEP our own implementations were used. For SCAILD we acquired the eigenvectors from PHONOPY, after which the displacements were generated for every normal mode according to a Gaussian distribution with the same mean-square displacement as given by theory for a classical harmonic oscillator at a constant temperature; that is, in Eq. (7), $\vec{d}$ is obtained from

$$\sigma_i^2 = \langle d_i^2 \rangle = \frac{k_B T}{\Omega_{i,i}^2}. \quad (12)$$

The sampling was from a classical distribution in order to be directly comparable to classical DFT molecular dynamics, although at the investigated temperatures we expect the effect on the results to be relatively small.

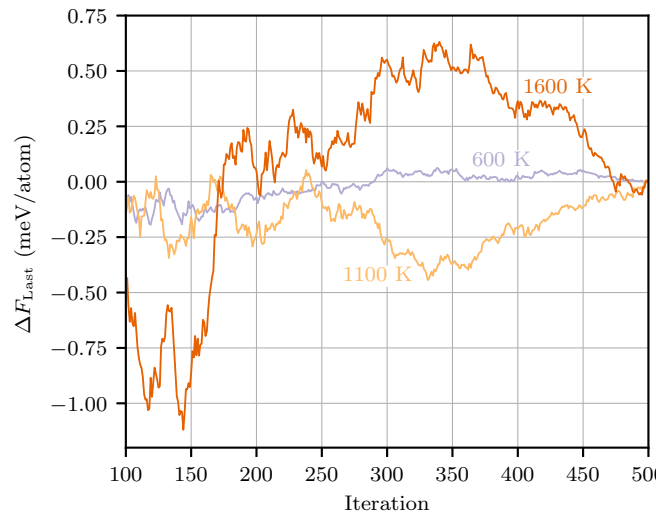

FIG. 3. Convergence of the free energy with respect to the number of iterations using SCAILD. The values are given as a difference from the last step. The free-energy difference between two consecutive iterations is typically orders of magnitude smaller than the longer-term changes.

As shown in Fig. 3 the changes in free energy between consecutive iterations can be orders of magnitude smaller than the changes over many iterations, so instead of basing the convergence on the former, we ran the simulations for a fixed number of (500) steps.

All the molecular dynamics simulations for TDEP were performed using Nosé-Hoover thermostating with the Nosé mass corresponding to approximately a time period of 80 fs and velocity Verlet integration with a time step of 1 fs. The symmetry requirements for the force constant matrix and crystal were taken into account when performing the linear fit of the displacement-force data. No additional cutoff distance in addition to that determined by the supercell was used for the force constants.

For both methods the simulations were done at 600, 1100, and 1600 K. At higher temperatures the oxygen atoms started migrating and occasionally created vacancy-interstitial pairs, which complicates the analysis not only for SCAILD and TDEP but also for the following thermodynamic integration which set the upper limit used in this work. The number of MD steps was 20 000 at 600 and 1100 K and 30 000 at 1600 K.

Thermodynamic integration was done for λ values of 0, 0.1, 0.25, 0.5, 0.75, 0.9, and 1. For TDEP $\lambda = 1$ data are already acquired before the fitting, and no extra calculation is needed. The same data were also used for SCAILD at $\lambda = 1$. For SCAILD at $\lambda = 0$ a separate fast MD run was done using the harmonic Hamiltonian, after which a subset of

uncorrelated samples was chosen for which the energy was calculated using DFT. Whereas a Nosé-Hoover thermostat was used for TDEP mostly because it automatically retains the position of the center of mass of the system and therefore simplifies the fitting, Langevin dynamics was used for the thermodynamic integration steps in order to avoid the possibility of incorrect sampling of the phase space when the system is close to harmonic [32]. The drift of the center of mass was not problematic for TI since only the energy differences were obtained instead of displacements.

All DFT calculations were done using VASP [33–36] with the projector augmented-wave method [37] with a plane wave cutoff energy of 400 eV and the generalized gradient approximation Perdew-Burke-Ernzerhof [38] exchange-correlation functional [39]. The number of electrons treated explicitly was 12 and 6 for Zr and O, respectively. A $2 \times 2 \times 2$ Monkhorst-Pack Γ-centered k-point grid [40] and Gaussian smearing with $\sigma = 0.05$ were used.

The choice for the k-point grid was based on the balance between sufficient accuracy and computational time. Fits for SCAILD and TDEP based on shorter runs with a $3 \times 3 \times 3$ Γ-centered grid at 1600 K resulted in a roughly 1 meV/atom difference. For thermodynamic integration a check was done by recalculating the $\lambda = 0.5$ point for TDEP at 1600 K using a $4 \times 4 \times 4$ Γ-centered grid. The difference seen was within the statistical uncertainty of the original calculation, so the UP-TILD [27] method was not applied.

As shown by Hellman [23], the relative errors in forces decrease by orders of magnitude as the magnitude of the forces increases to that of the thermally excited states. Based on that, the 0 K harmonic calculations, including obtaining the eigenvectors for SCAILD, were done using a denser $7 \times 7 \times 7$ k-point grid.

III. RESULTS

The vibrational free energies calculated using all of the methods are shown in Table I. The full anharmonic vibrational free energies are in good agreement. Even at the highest considered temperature, 1600 K, all stratified free-energy perturbation and thermodynamic integration results are within 1 meV/atom. Both SCAILD and TDEP are, however, off by about 20 meV/atom, and perhaps surprisingly, even the free energy calculated from harmonic lattice dynamics is a lot closer to the value obtained from thermodynamic integration than those of either effective harmonic method.

The errors in free energies predicted by SCAILD and TDEP are opposite in sign. This is also evident from the thermodynamic integration results shown in Fig. 4. Since the TDEP force constant matrix is fitted to the DFT-MD results, the average potential energy difference between DFT and TDEP is also minimal at $\lambda = 1$. It is also seen that setting the average potential energies to be equal, as done in Ref. [11] [Eq. (21)], would do little to reduce the error. In this case the whole TI curve would be shifted down by roughly 3 meV/atom for the temperature of 1600 K, which accounts for only 15% of the total error. Similar conclusions can be drawn for SCAILD, for which the agreement with DFT is best at $\lambda = 0$, with the error due to mismatched average potential energies being slightly larger and, if taken into account, providing a better estimation for the full vibrational free energy than TDEP.

TABLE I. Vibrational free energies (in meV/atom) calculated by different methods. The meaning of the acronyms is as follows: LD, lattice dynamics; H, harmonic; EH, effective harmonic; AH, anharmonic; FEP, free-energy perturbation; SFEP, stratified free-energy perturbation; TI, thermodynamic integration. For TDEP the EH results are presented for both temperature-independent and temperature-dependent eigenvectors, denoted by Q_0 and Q_T, respectively.

Method	Type	600 K	1100 K	1600 K
LD	H	4.0	−176.7	−415.9
SCAILD	EH	7.1	−167.3	−398.0
	AH, FEP	4.1	−176.4	−415.1
	AH, SFEP	3.8	−177.9	−419.0
	AH, TI	3.8	−178.1	−419.1
TDEP	EH, Q_0	0.9	−186.8	−438.5
	EH, Q_T	1.0	−186.6	−437.9
	AH, FEP	3.2	−180.1	−422.0
	AH, SFEP	3.4	−177.8	−418.4
	AH, TI	3.5	−177.7	−418.6

Free-energy perturbation was not able to correct all of the discrepancy, possibly due to the limited number of samples; however, the stratified version gives free energies that agree very well with TI results. This is expected since the same input data were used for both methods.

In either case shifting the potential energy does not result in a change in the force constants or in the phonon dispersions, which are shown in Fig. 5 for TDEP and Fig. 6 for SCAILD. The general trend is for TDEP to predict a decrease and for SCAILD to predict an increase in frequencies over

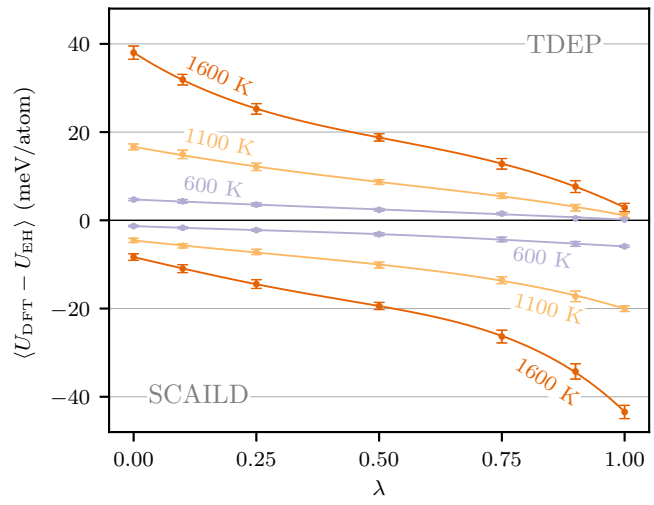

FIG. 4. Thermodynamic integration results for TDEP and SCAILD. Every dot corresponds to one equilibrium MD calculation with a λ-mixed Hamiltonian. The error bars were obtained using the block-averaging method and are shown for ±3 standard deviations. The solid line is a fourth-order polynomial fit with the reciprocals of the standard deviations used as weights.

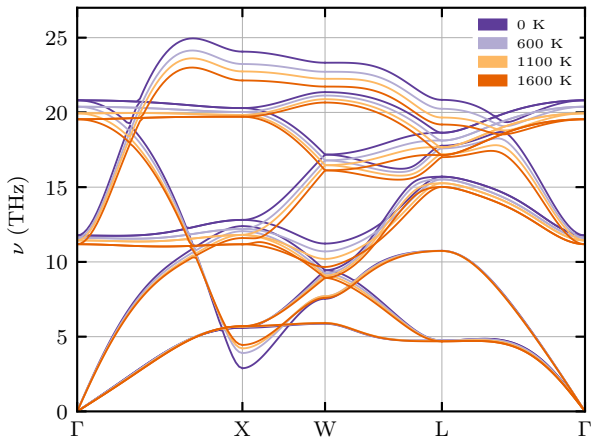

FIG. 5. Phonon dispersion dependence on temperature as predicted by TDEP.

all of the reciprocal space. A notable exception to that is the lowest-frequency mode at the X point, which would be unstable without the external pressure. Both methods predict an increase in the frequency, albeit SCAILD from 2.9 THz at 0 K to 6.1 THz and TDEP to 4.4 THz at 1600 K. The changes in frequencies at high-symmetry q points are depicted in Fig. 7. We must note that since the calculations were done at a fixed volume, the typical lowering of the frequencies due to thermal expansion is not taken into account.

The reason why TDEP, at least when up to second-order force constants are considered, cannot provide a better estimate than SCAILD is that an effective harmonic Hamiltonian fitted at either $\lambda = 0$ or $\lambda = 1$ exhibits similar nontransferability. Whereas the average energy difference between DFT and the effective harmonic model can be forced to be zero at one of the end points of the TI curve, its absolute value can only monotonically increase as TI is performed, and the sampled atomic configurations will start to differ from those used for the fit. This can be proven using the Gibbs-Bogoliubov inequality [41], which states that

$$\left(\frac{\partial^2 F}{\partial \lambda^2}\right)_{NVT} \leqslant 0. \tag{13}$$

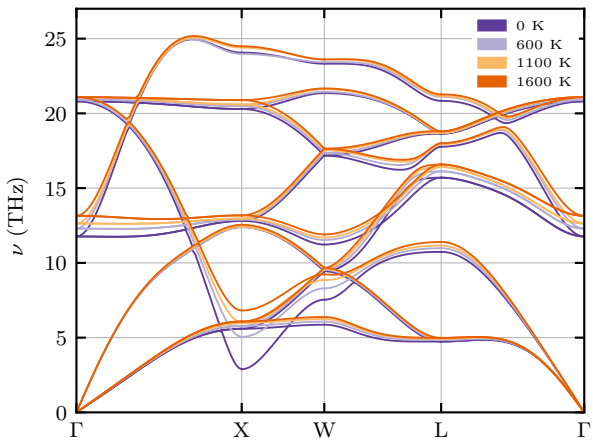

FIG. 6. Phonon dispersion dependence on temperature as predicted by SCAILD.

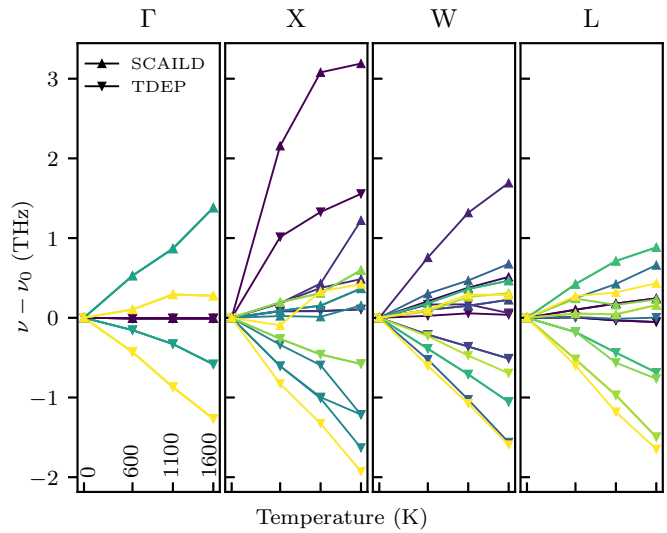

FIG. 7. Temperature dependence of change in phonon mode frequencies at high-symmetry points. The darker and lighter colors indicate lower and higher initial frequencies, respectively.

As the anharmonicity increases, the transferability and thus the estimate for the full vibrational free energy become worse. This can also be explained as follows: let us consider a full infinite expansion of the DFT Hamiltonian. Starting from a harmonic model, we carry out the TDEP process, that is, perform molecular dynamics runs at $\lambda = 1$, and for each subsequent run we increase the number of terms in the expansion. For up to a quadratic term the effective harmonic model can be fitted exactly, and $\Delta U = 0$ for any λ. As we add more terms, ΔU at $\lambda = 0$ starts to deviate from zero more and more while being kept zero at $\lambda = 1$. Whereas lattice dynamics ignores terms higher than second order, both SCAILD and TDEP incorporate those in an effective manner into the harmonic Hamiltonian, and as shown, this can lead to a much larger error. In addition, it is not obvious that adding, for example, the third-order force constants to the effective model Hamiltonian necessarily reduces the error since the second-order force constants may remain relatively unaffected.

IV. CONCLUSIONS

Given temperature-independent eigenvectors, the effective harmonic models obtained through either SCAILD or TDEP produce two types of systematic errors. One is due to the different choices of the ensemble of displacements and forces used to fit the data. Based on our results neither could be considered better than the other, the reason being that in either case it is not the remaining explicitly anharmonic energy obtained through thermodynamic integration that is minimized, but the potential energy difference at one of the end points of the λ-integration curve. The other systematic error, common to both, is introduced by trying to reproduce the anharmonic interactions in an effective harmonic manner.

The free energies predicted by either method diverge as the temperature increases, with the general trend being SCAILD predicting an increase in the phonon frequencies

and higher free energy than the exact value, as opposed to TDEP, which predicts decreasing frequencies and lower free energy. For the system considered in this work both give a worse estimate of the free energy than the 0 K harmonic model. Therefore, relying on one or the other can introduce large errors when investigating the vibrational thermodynamic properties of materials, especially when the results of either are compared with those obtained through other methods, for example, when using the quasiharmonic approximation to calculate the free energy of one phase but one of the effective harmonic methods for another in order to compute the phase stability. In addition, due to the nonlinearity of the systematic error with respect to temperature, it is possible that the error in other thermodynamic quantities derived from free energy, such as heat capacity, will have even larger errors. Free-energy perturbation can be used without extra computational cost in order to estimate the error, but since it may not account for all of the difference between the approximate and true free energy, thermodynamic integration or any other method that takes all of the anharmonicity explicitly into account has to be used.

ACKNOWLEDGMENTS

The research leading to these results has received funding from the Swedish Centre for Nuclear Technology (SKC). Computational resources were provided by Swedish National Infrastructure for Computing (SNIC). Comments by A. Samanta and A. Tamm from Lawrence Livermore National Laboratory are greatly appreciated.

[1] B. Fultz, Prog. Mater. Sci. **55**, 247 (2010).
[2] A. Togo and I. Tanaka, Scr. Mater. **108**, 1 (2015).
[3] F. W. de Wette, L. H. Nosanow, and N. R. Werthamer, Phys. Rev. **162**, 824 (1967).
[4] K. Parlinski, Z. Q. Li, and Y. Kawazoe, Phys. Rev. Lett. **78**, 4063 (1997).
[5] P. Souvatzis, O. Eriksson, M. I. Katsnelson, and S. P. Rudin, Phys. Rev. Lett. **100**, 095901 (2008).
[6] A. van de Walle, Q. Hong, S. Kadkhodaei, and R. Sun, Nat. Commun. **6**, 7559 (2015).
[7] S. Kadkhodaei, Q.-J. Hong, and A. van de Walle, Phys. Rev. B **95**, 064101 (2017).
[8] P. Souvatzis and S. P. Rudin, Phys. Rev. B **78**, 184304 (2008).
[9] P. Souvatzis, O. Eriksson, M. I. Katsnelson, and S. P. Rudin, Comput. Mater. Sci. **44**, 888 (2009).
[10] O. Hellman, I. A. Abrikosov, and S. I. Simak, Phys. Rev. B **84**, 180301(R) (2011).
[11] O. Hellman, P. Steneteg, I. A. Abrikosov, and S. I. Simak, Phys. Rev. B **87**, 104111 (2013).
[12] I. Mosyagin, O. Hellman, W. Olovsson, S. I. Simak, and I. A. Abrikosov, J. Phys. Chem. A **120**, 8761 (2016).
[13] W. Kohn and L. J. Sham, Phys. Rev. **140**, A1133 (1965).
[14] B. Grabowski, T. Hickel, and J. Neugebauer, Phys. Status Solidi B **248**, 1295 (2011).
[15] M. Palumbo, B. Burton, A. Costa e Silva, B. Fultz, B. Grabowski, G. Grimvall, B. Hallstedt, O. Hellman, B. Lindahl, A. Schneider, P. E. A. Turchi, and W. Xiong, Phys. Status Solidi B **251**, 14 (2014).
[16] S. G. Moustafa, A. J. Schultz, and D. A. Kofke, Phys. Rev. E **92**, 043303 (2015).
[17] S. G. Moustafa, A. J. Schultz, and D. A. Kofke, J. Chem. Theory Comput. **13**, 825 (2017).
[18] B. Grabowski, P. Söderlind, T. Hickel, and J. Neugebauer, Phys. Rev. B **84**, 214107 (2011).
[19] B. Grabowski, Y. Ikeda, F. Körmann, C. Freysoldt, A. I. Duff, A. Shapeev, and J. Neugebauer, arXiv:1902.11230.
[20] P. Korotaev, M. Belov, and A. Yanilkin, Comput. Mater. Sci. **150**, 47 (2018).
[21] A. A. Maradudin and S. H. Vosko, Rev. Mod. Phys. **40**, 1 (1968).
[22] F. Ercolessi and J. B. Adams, Europhys. Lett. **26**, 583 (1994).
[23] O. Hellman, Ph.D. thesis, Linköping University, 2012.
[24] M. de Koning and A. Antonelli, Phys. Rev. E **53**, 465 (1996).
[25] R. Freitas, M. Asta, and M. de Koning, Comput. Mater. Sci. **112**, 333 (2016).
[26] S. Ryu and W. Cai, Modell. Simul. Mater. Sci. Eng. **16**, 085005 (2008).
[27] B. Grabowski, L. Ismer, T. Hickel, and J. Neugebauer, Phys. Rev. B **79**, 134106 (2009).
[28] A. Glensk, B. Grabowski, T. Hickel, and J. Neugebauer, Phys. Rev. Lett. **114**, 195901 (2015).
[29] A. I. Duff, T. Davey, D. Korbmacher, A. Glensk, B. Grabowski, J. Neugebauer, and M. W. Finnis, Phys. Rev. B **91**, 214311 (2015).
[30] A. Pohorille, C. Jarzynski, and C. Chipot, J. Phys. Chem. B **114**, 10235 (2010).
[31] M. Sternik and K. Parlinski, J. Chem. Phys. **123**, 204708 (2005).
[32] G. J. Martyna, M. L. Klein, and M. Tuckerman, J. Chem. Phys. **97**, 2635 (1992).
[33] G. Kresse and J. Hafner, Phys. Rev. B **47**, 558 (1993).
[34] G. Kresse and J. Hafner, Phys. Rev. B **49**, 14251 (1994).
[35] G. Kresse and J. Furthmuller, Comput. Mater. Sci. **6**, 15 (1996).
[36] G. Kresse and J. Furthmüller, Phys. Rev. B **54**, 11169 (1996).
[37] G. Kresse and D. Joubert, Phys. Rev. B **59**, 1758 (1999).
[38] J. P. J. Perdew, K. Burke, and M. Ernzerhof, Phys. Rev. Lett. **77**, 3865 (1996).
[39] J. P. Perdew, K. Burke, and M. Ernzerhof, Phys. Rev. Lett. **78**, 1396 (1997).
[40] H. Monkhorst and J. Pack, Phys. Rev. B **13**, 5188 (1976).
[41] D. Frenkel and B. Smit, *Understanding Molecular Simulation* (Academic Press, San Diego, 2002).